# Measurements of $t\bar{t}$ pairs produced in association with electroweak gauge bosons using the ATLAS detector


Alvaro Lopez Solis

*On behalf of the ATLAS collaboration*


EPS Conference – High Energy Physics 2019
10th – 17th July 2019

# Overview

- Very successful Run II of the LHC during the last three years (2015-2018) at √s= 13 TeV.
- ATLAS recorded a dataset of 139 $fb^{-1}$. Around seven times larger than the previous Run I at √s= 8 TeV (20.3 $fb^{-1}$).
- Reaching ‹μ› = 33.7 for the combined whole Run II.

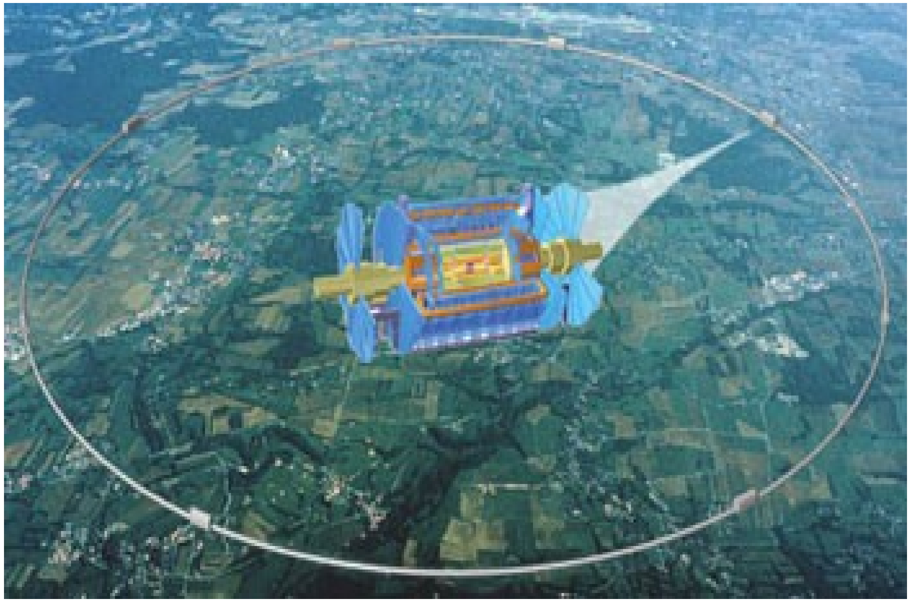

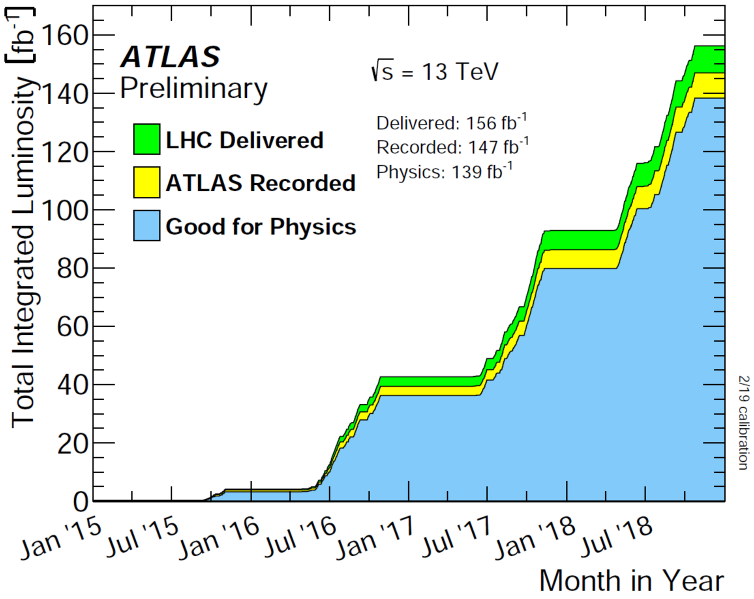


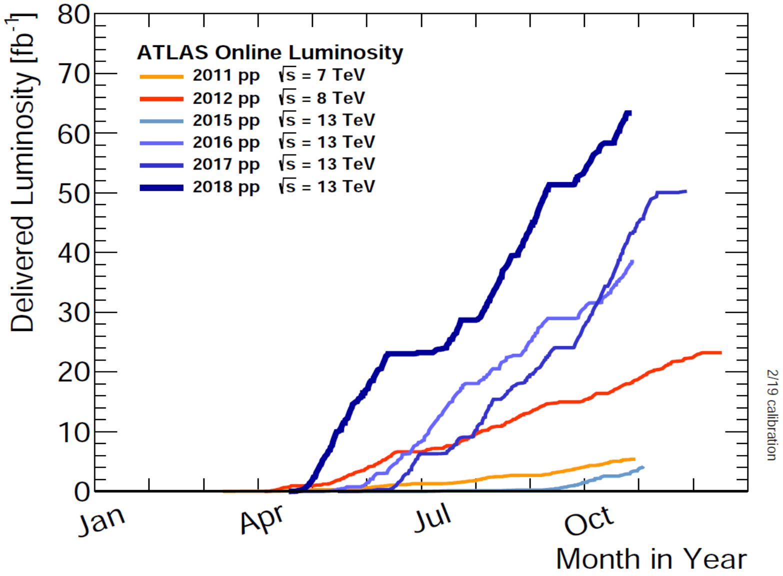

# Status of ttV and ttγ measurements

- I will focus today in the latest results published by the ATLAS collaboration using the 2015+2016 recorded data (36.1 $fb^{-1}$) for $t\bar{t}$ produced in association with an electroweak boson

*ATLAS Top Summary plots*

*$t\bar{t}Z$ and $t\bar{t}W$: cross-section measurement*

*Phys. Rev. D 99 (2019) 072009*

*$t\bar{t}+\gamma$: fiducial and differential cross-section*

*Eur. Phys. J. C 79 (2019) 382*

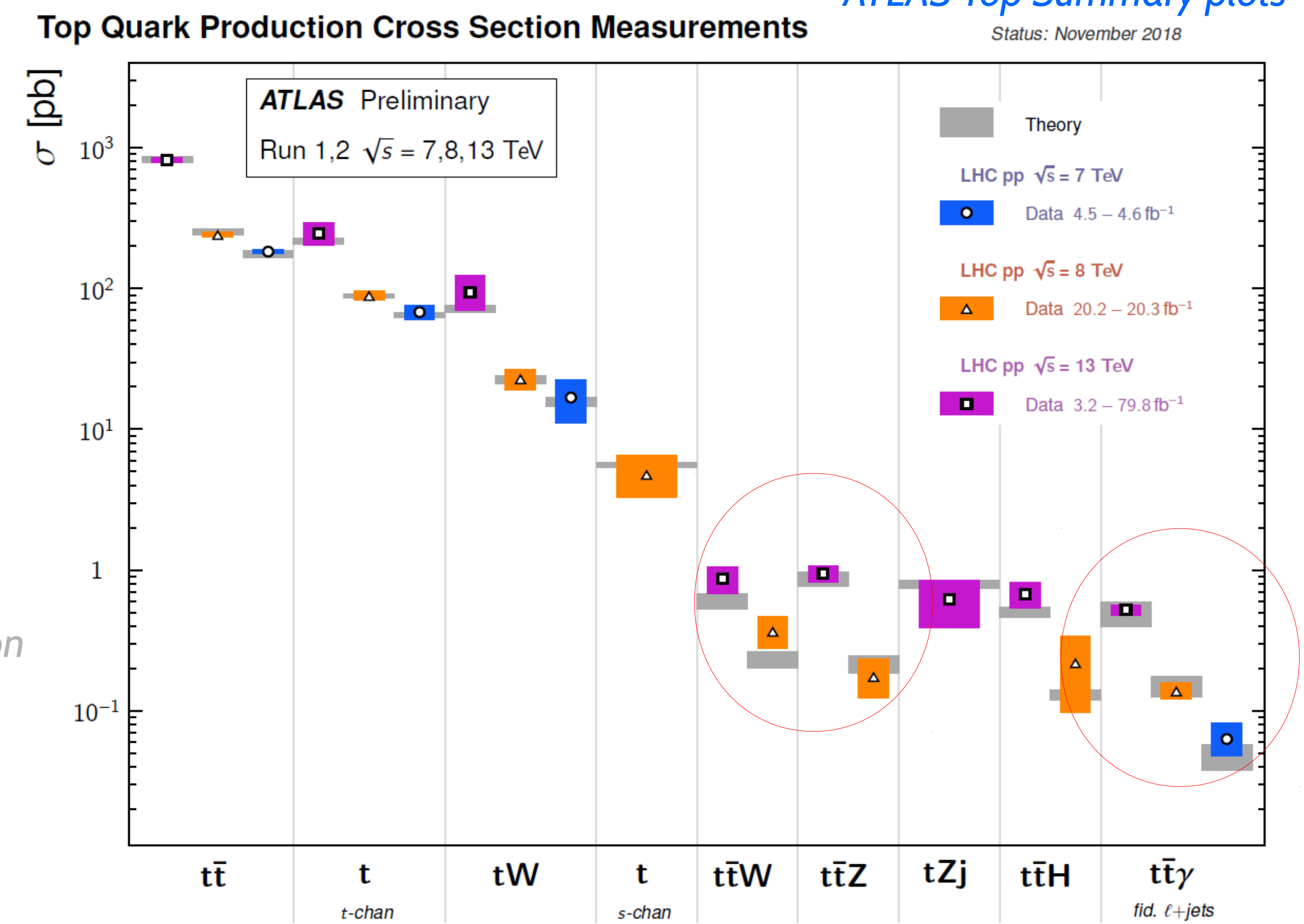


Updated results with full luminosity (139 $fb^{-1}$) are in progress

# Motivation

- Direct probe of the weak couplings of the top to W/ Z and photons.
- Deviations from the SM model predictions can probe beyond SM scenarios:
  - These final states are sensitive to anomalous couplings of the top and photons and/or $t\bar{t}$ spin correlation and charge asymmetry amongst others.
- Differential measurements improve Monte-Carlo modelling.
- In addition, these processes are important backgrounds for other SM/BSM searches in ATLAS.

*$t\bar{t}H$ multilepton in ATLAS: PhysRevD.97.072003*

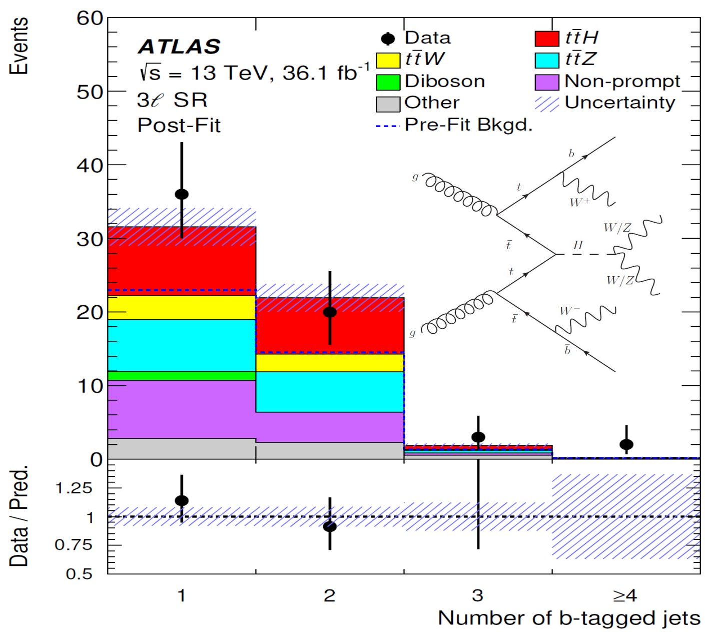


*Stop pair production in 0 lepton final state: JHEP12(2017)085*

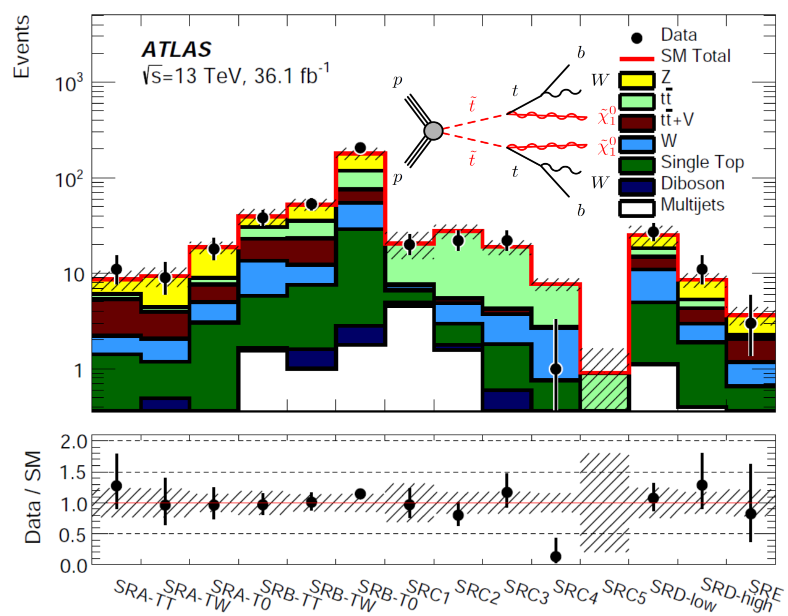

Eur. Phys. J. C 79 (2019) 382

# $t\bar{t}\gamma$ fiducial and differential cross-section
# 13 TeV, 36.1 fb$^{-1}$

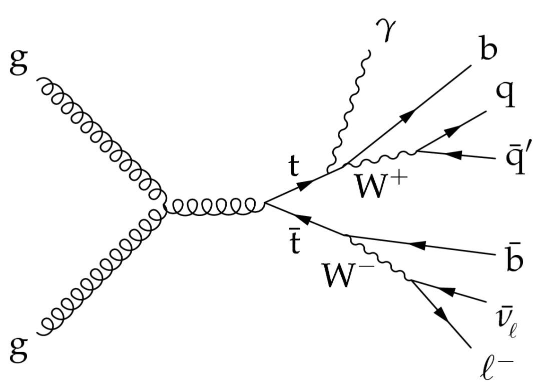


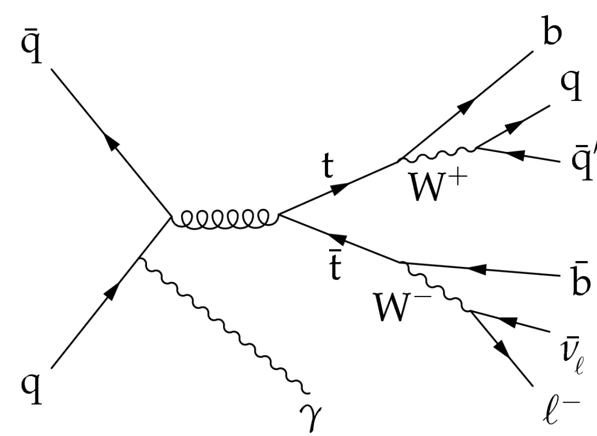

# Analysis overview

- Targetting semileptonic and dileptonic decays of the ttbar system.
  - $t\bar{t}$/Z+jets: jets and electrons faking photons and jets faking electrons.
  - Wγ (Zγ): irreducible background single lepton (dilepton) channel.
- Prompt photon tagger in single lepton channel to discriminate fake photons from prompt.

| Channel | Single lepton | Dilepton |
|---|---|---|
| $t\bar{t}\gamma$ | 6 490 ± 420 | 720 ± 34 |
| Hadronic-fake | 1 440 ± 290 | 49 ± 27 |
| Electron-fake | 1 650 ± 170 | 2 ± 1 |
| Fake lepton | 360 ± 200 | – |
| $W\gamma$ | 1 130 | |
| $Z\gamma$ | | 75 ± 52 |
| Other prompt | 690 ± 260 | 18 ± 7 |
| Total | 11 750 ± 710 | 863 ± 78 |
| Data | 11 662 | 902 |

- Event level discriminator (ELD) to separate signal and background.
  - Neural network on Keras → Output provide strong discrimination between signal/background.
- Fiducial cross-section measurements fitting ELD shape.

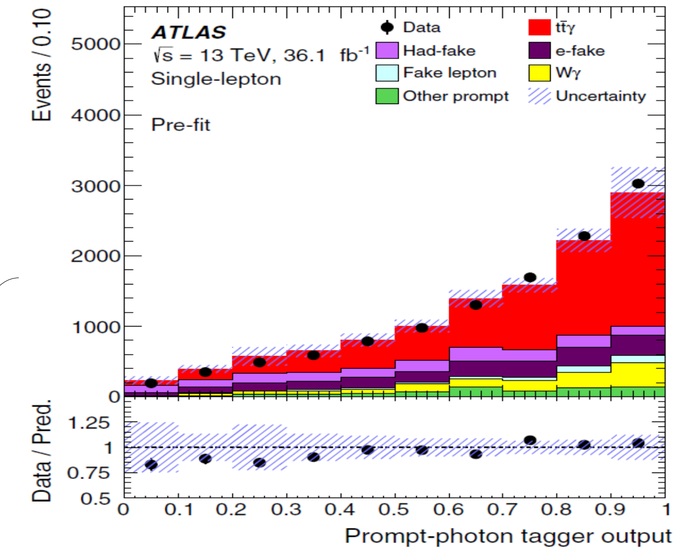


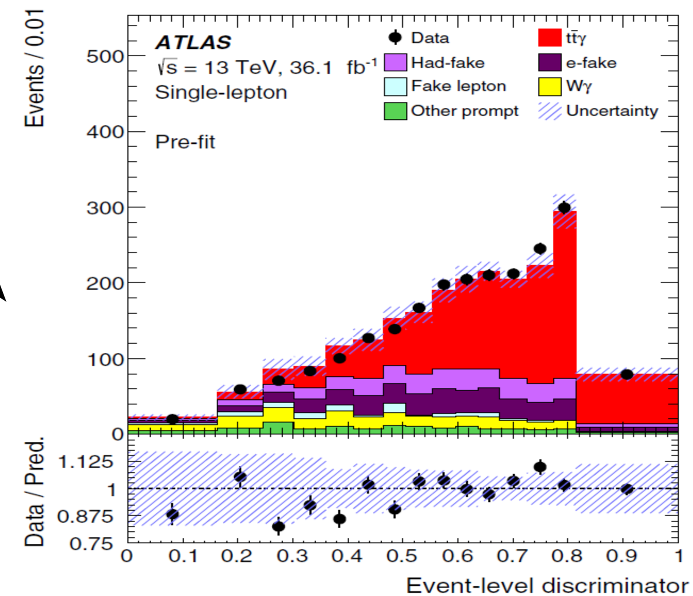

# Fiducial cross-section measurement

- Results derived with a shape fit of the ELD in the single-lepton and dilepton channels.
- Individual and combined fits to different flavor channels.
- Results compatible with dedicated NLO in QCD predictions in this fiducial region from authors of arXiv:1102.1967.

$$\sigma_{\mathrm{fid}}^{\mathrm{SL}} = 521 \pm 9(\mathrm{stat.}) \pm 41(\mathrm{sys.})\ \mathrm{fb} \qquad \sigma_{\mathrm{fid}}^{\mathrm{DL}} = 69 \pm 3(\mathrm{stat.}) \pm 4(\mathrm{sys.})\ \mathrm{fb}$$

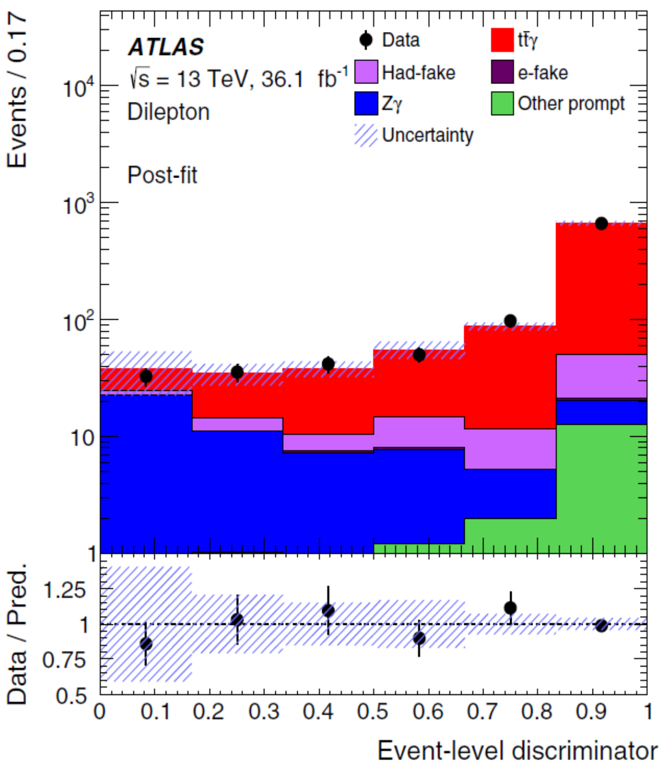


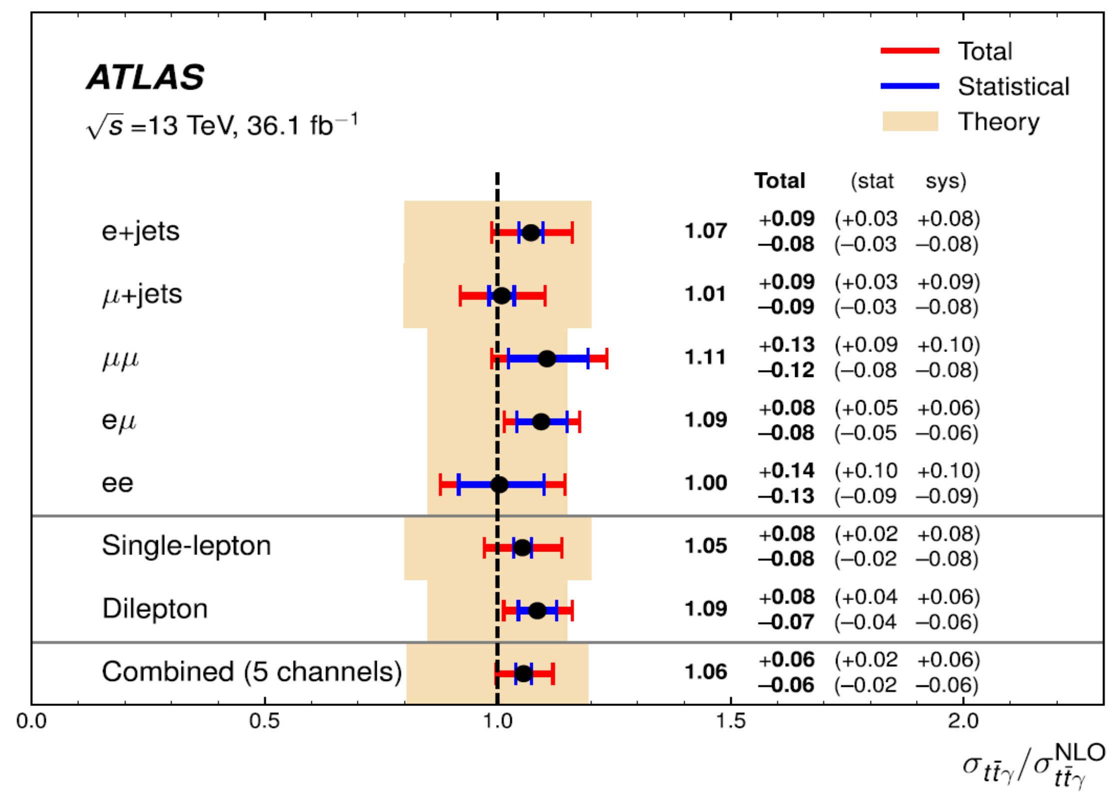

# Differential cross-section results

- Iterative Bayesian unfolding technique to obtain particle-level measurements.
- Overall agreement between the unfolded results and the compared generators, modelling ttγ at LO.
  - Largest disagreement → 1.5 σ in the Δϕ(l+,l-).
- Modelling of the Powheg+Py8 ttbar sample with prompt-photon radiation shows softer photon than in data.

$$\sigma_k = \frac{1}{L} \times \frac{1}{\epsilon_k} \times \sum_j M^{-1}_{jk} \times \left(N^{\text{obs}}_j - N^b_j\right) \times (1 - f_{\text{out},j})$$

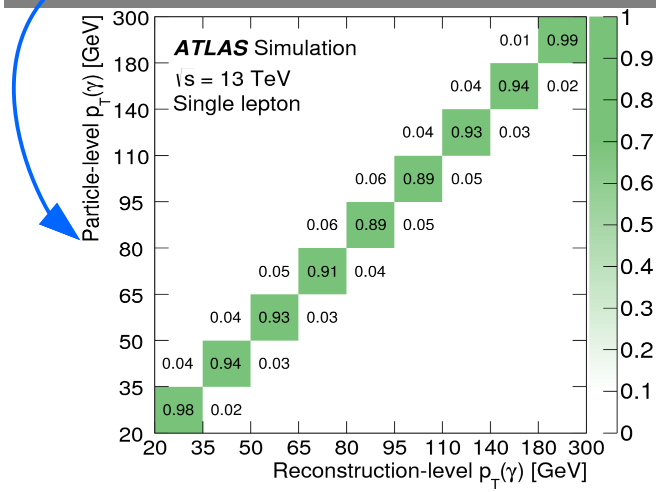


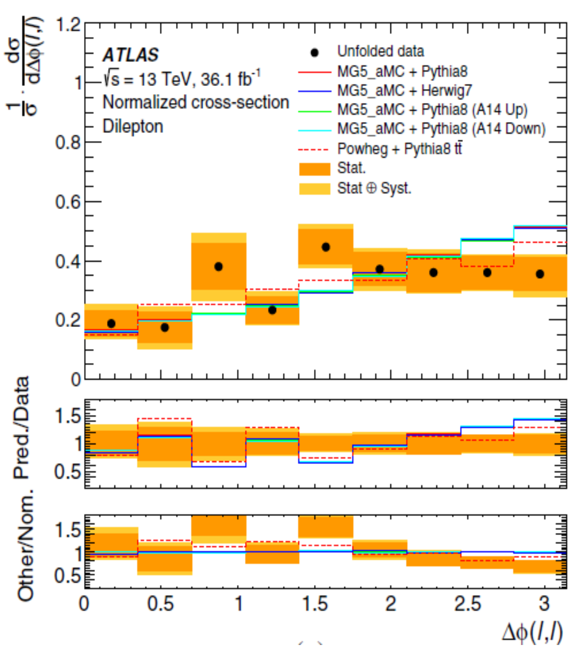


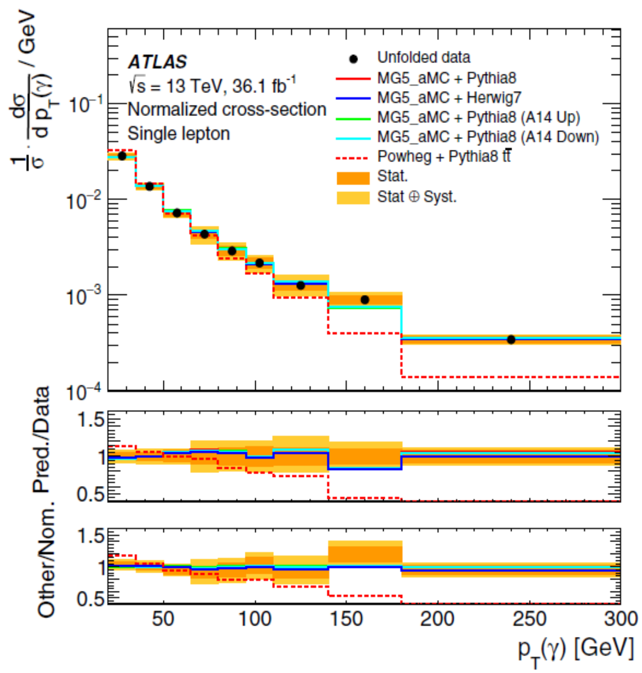


Dominated by tt (Zγ) modelling and statistics in single-lepton (dilepton)

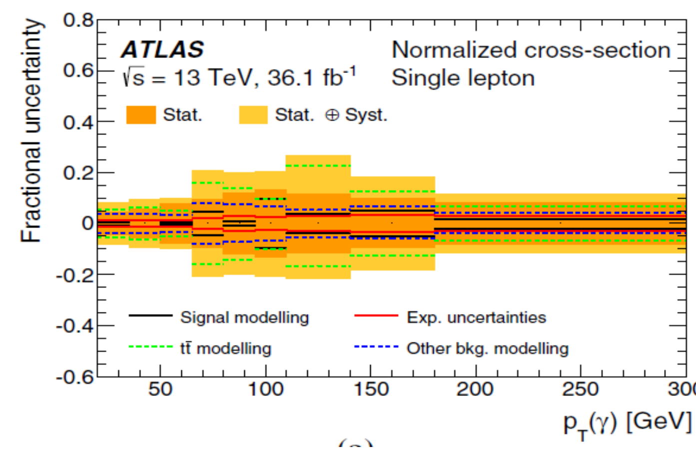

Phys. Rev. D 99 (2019) 072009

# $t\bar{t}Z$ and $t\bar{t}W$ cross-section measurement 13TeV, 36.1fb$^{-1}$

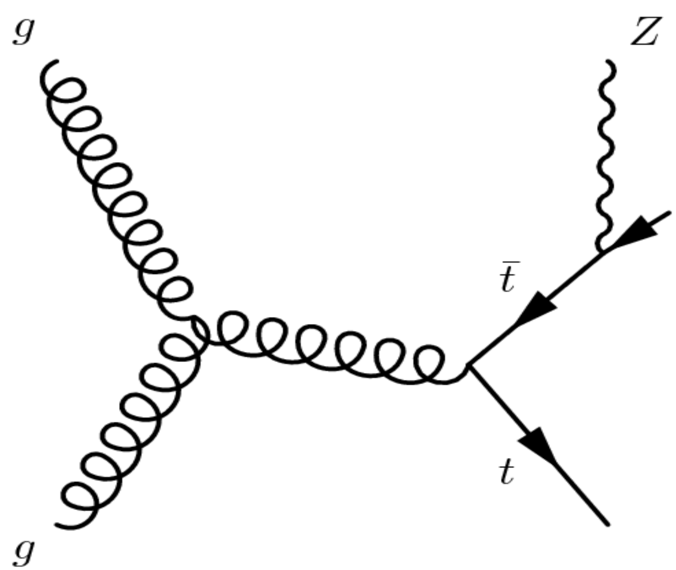


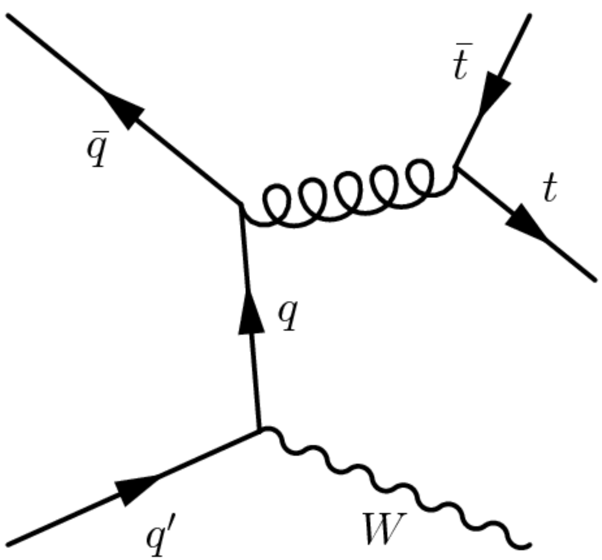

# Analysis overview: $t\bar{t}W$

- 2 lepton same-sign signal regions (2l-SS):
  - Targetting W → lν and semileptonic tt system.
  - Dominated by fake-lepton and charge-flip.
- 3 lepton signal region:
  - Targetting leptonic decays of all W-bosons in the event.
  - Z-veto on opposite sign same flavour leptons.
- Multivariate techniques to reduce fake-lepton backgrounds. Data-driven fake-lepton and charge flip estimation.
- Multi-bin fit to all SRs and CRs.

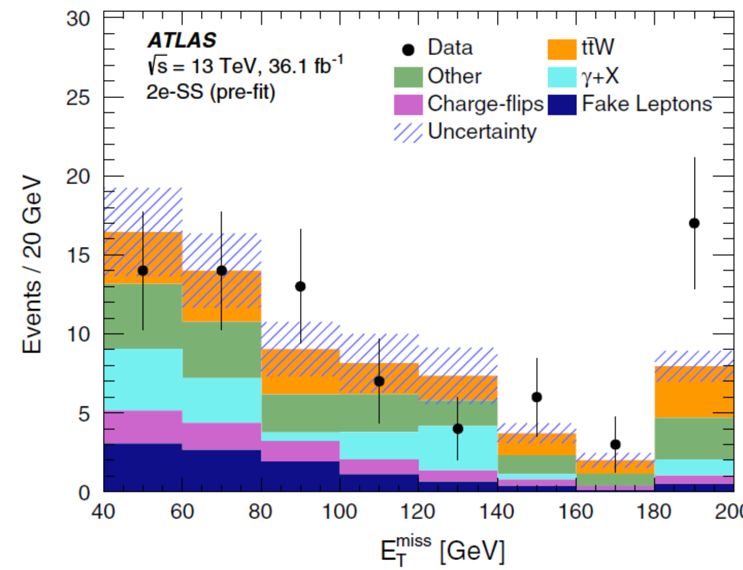


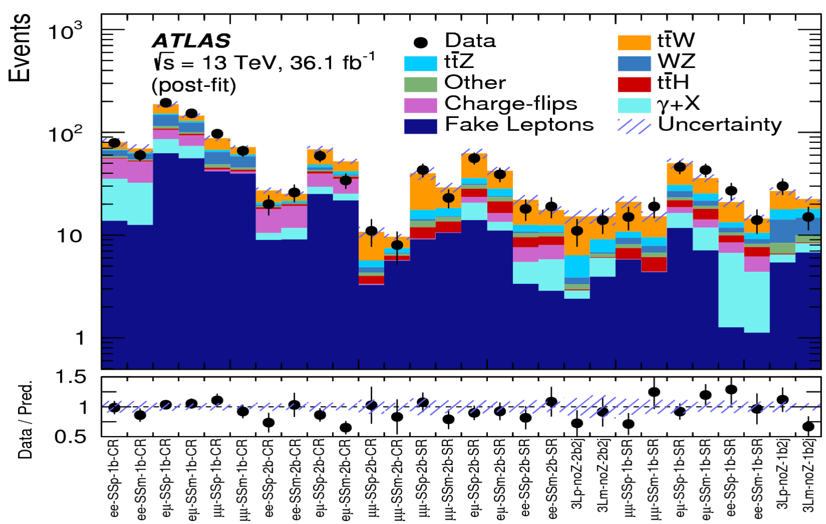


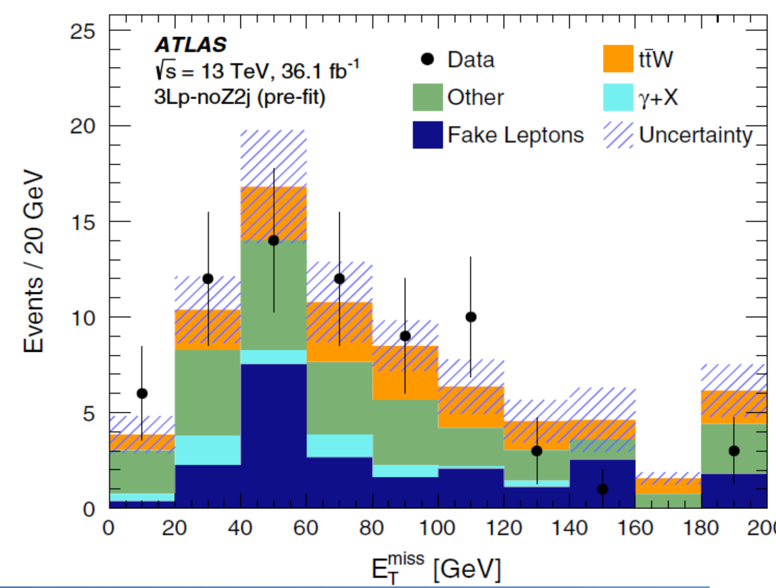

# Analysis overview: $t\bar{t}Z$

- Regions targetting 2L,3L (most sensitive) and 4L (high purity).
- Dedicated control regions for the dominant backgrounds in each channel:
  - 2L: $t\bar{t}$ and Z+jets. Z+jets sample classified by heavy-flavour (b- and c-hadron) mutliplicity.
  - 3L: WZ control region. Other backgrounds from MC.
  - 4L: ZZ control region. Other backgrounds from MC.
- BDT fit to 2L region and multi-bin fit in 3L,4L regions.

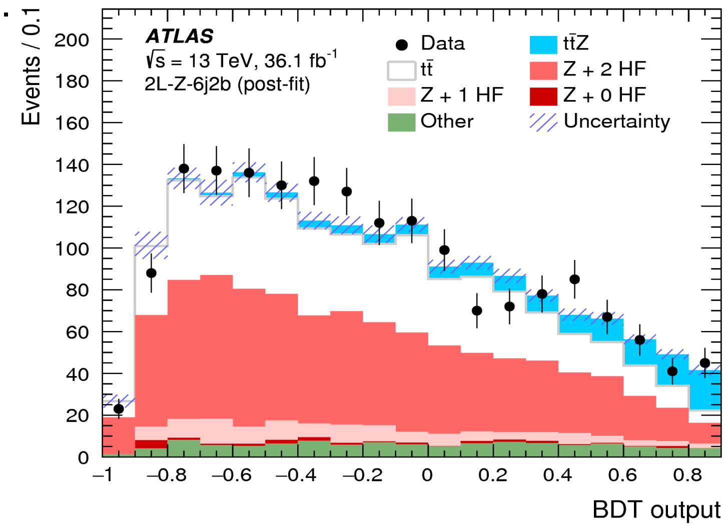


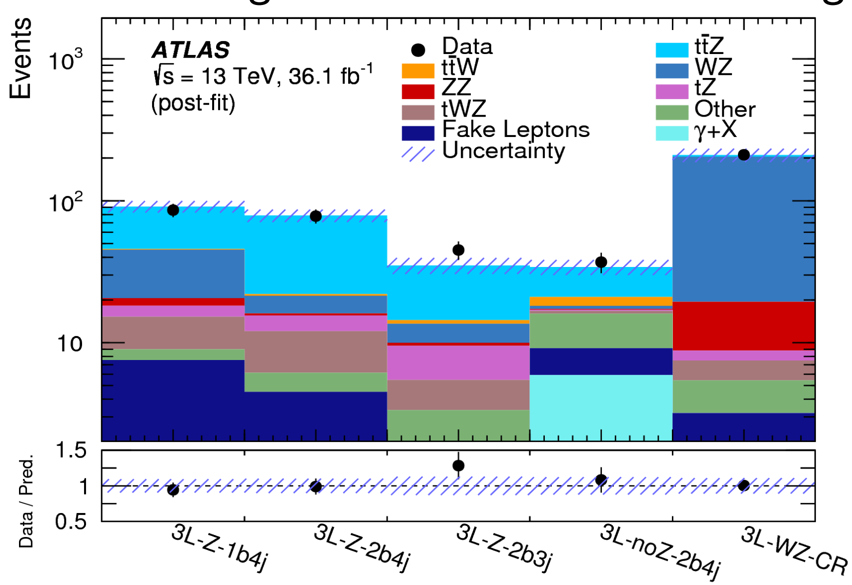


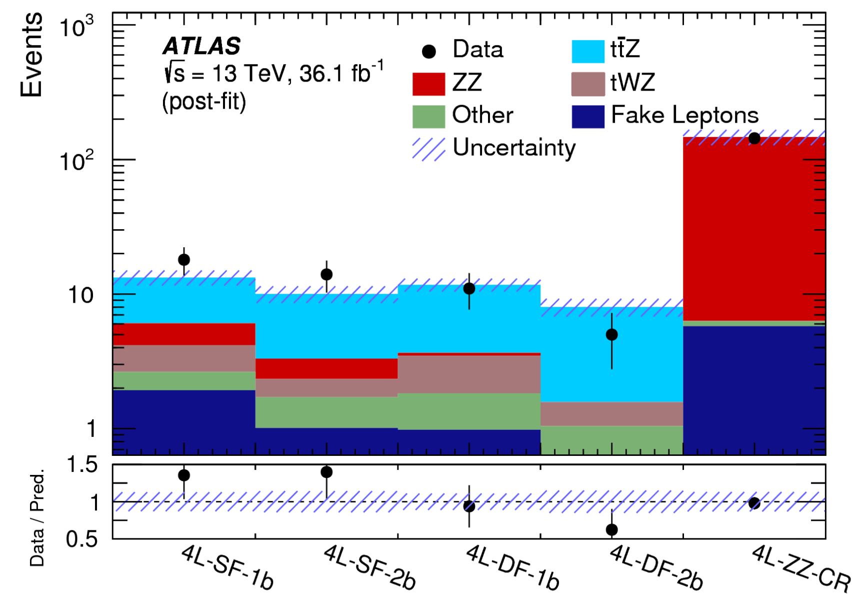

# Measurement of the ttZ/ttW cross-section

- Combined fit in all signal regions to simultaneous substraction of $\sigma_{ttZ}$ and $\sigma_{ttW}$.
- Substracted values compatible within uncertainties to individual fits.
- Dominated by signal modelling and flavour-tagging/jet uncertainties.

$$\sigma_{t\bar{t}Z} = 0.95 \pm 0.08_{\text{stat}} \pm 0.10_{\text{syst}}\ \text{pb}$$

$$\sigma_{t\bar{t}W} = 0.87 \pm 0.13_{\text{stat}} \pm 0.14_{\text{syst}}\ \text{pb}$$

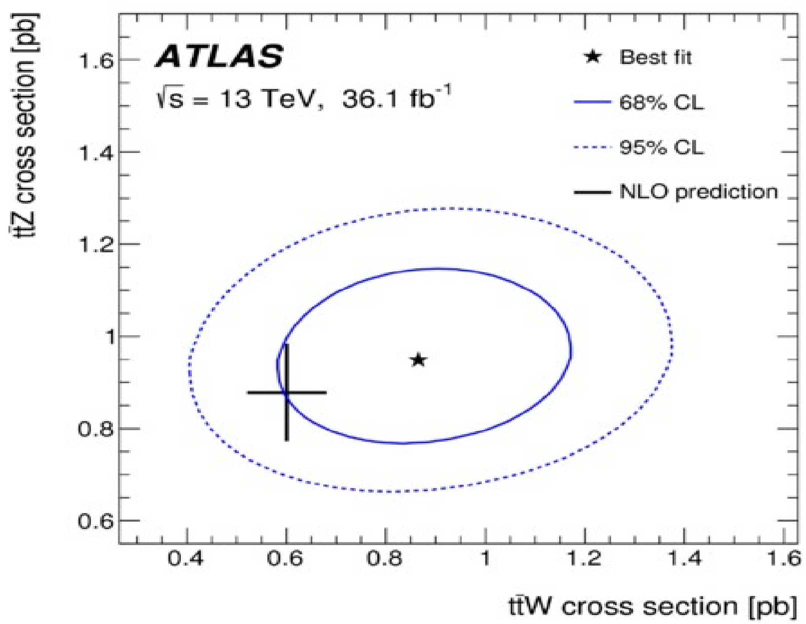


| Fit configuration | $\mu_{t\bar{t}Z}$ | $\mu_{t\bar{t}W}$ |
|---|---|---|
| Combined | $1.08 \pm 0.14$ | $1.44 \pm 0.32$ |
| $2\ell$-OS | $0.73 \pm 0.28$ | ··· |
| $3\ell\, t\bar{t}Z$ | $1.08 \pm 0.18$ | ··· |
| $2\ell$-SS and $3\ell\, t\bar{t}W$ | ··· | $1.41 \pm 0.33$ |
| $4\ell$ | $1.21 \pm 0.29$ | ··· |

| Uncertainty | $\sigma_{t\bar{t}Z}$ | $\sigma_{t\bar{t}W}$ |
|---|---|---|
| Luminosity | 2.9% | 4.5% |
| Simulated sample statistics | 2.0% | 5.3% |
| Data-driven background statistics | 2.5% | 6.3% |
| JES/JER | 1.9% | 4.1% |
| Flavor tagging | 4.2% | 3.7% |
| Other object-related | 3.7% | 2.5% |
| Data-driven background normalization | 3.2% | 3.9% |
| Modeling of backgrounds from simulation | 5.3% | 2.6% |
| Background cross sections | 2.3% | 4.9% |
| Fake leptons and charge misID | 1.8% | 5.7% |
| $t\bar{t}Z$ modeling | 4.9% | 0.7% |
| $t\bar{t}W$ modeling | 0.3% | 8.5% |
| Total systematic | 10% | 16% |
| Statistical | 8.4% | 15% |
| Total | 13% | 22% |

Compatible with 68% CL with ttZ/ttW NLO predictions.

# Top EFT constraints

- Constraints on 5 Top EFT Wilson coefficients with ATLAS results. Coefficients related only to the ttZ vertex : *Reference SMEFT paper*
- Using the 3L and 4L signal regions. Discard 2L OS due to its low purity.

| Operator | Expression |
|---|---|
| $\mathcal{O}_{\phi Q}^{(3)}$ | $(\phi^\dagger i\overset{\leftrightarrow}{D}{}^I_\mu\phi)(\bar{Q}\gamma^\mu\tau^I Q)$ |
| $\mathcal{O}_{\phi Q}^{(1)}$ | $(\phi^\dagger i\overset{\leftrightarrow}{D}_\mu\phi)(\bar{Q}\gamma^\mu Q)$ |
| $\mathcal{O}_{\phi t}$ | $(\phi^\dagger i\overset{\leftrightarrow}{D}_\mu\phi)(\bar{t}\gamma^\mu t)$ |
| $\mathcal{O}_{tW}$ | $(\bar{Q}\sigma^{\mu\nu}\tau^I t)\tilde{\phi}W^I_{\mu\nu}$ |
| $\mathcal{O}_{tB}$ | $(\bar{Q}\sigma^{\mu\nu}t)\tilde{\phi}B_{\mu\nu}$ |

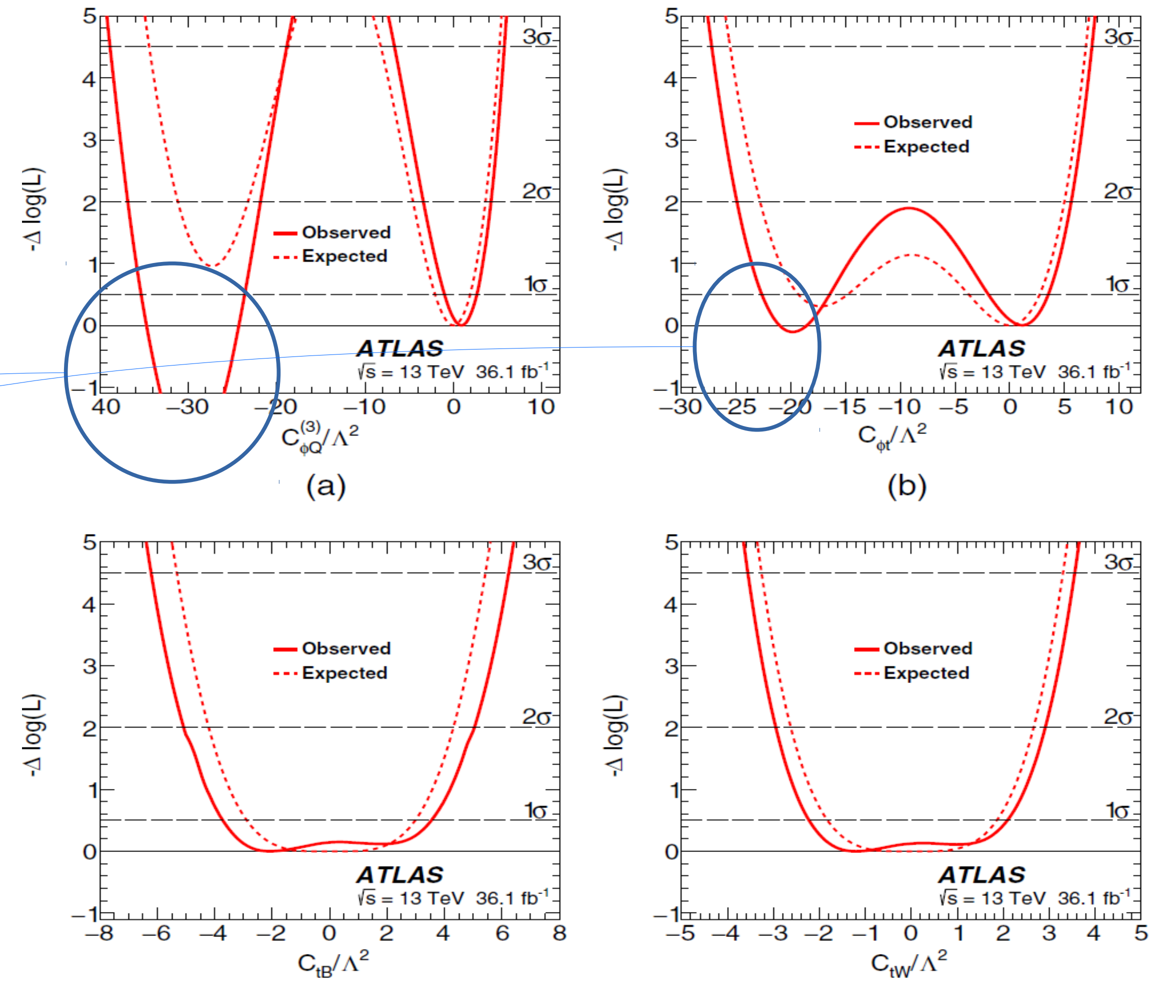


Rejected by previous constraints

| Coefficients | $C^{(3)}_{\phi Q}/\Lambda^2$ | $C_{\phi t}/\Lambda^2$ |
|---|---|---|
| Previous indirect constraints at 68% C.L. | $[-4.7, 0.7]$ | $[-0.1, 3.7]$ |
| Previous direct constraints at 95% C.L. | $[-1.3, 1.3]$ | $[-9.7, 8.3]$ |

# Conclusion

- Several results from using 2015 and 2016 ATLAS dataset have been published on $t\bar{t}$ production in association with electroweak bosons.
- ATLAS have published two results with 36.1 $fb^{-1}$ data:
  - Measurements of inclusive and differential fiducial cross-sections of $t\bar{t}\gamma$ production in leptonic final states at $\sqrt{s}$= 13 TeV in ATLAS
  - Measurement of the $t\bar{t}Z$ and $t\bar{t}W$ cross sections in proton-proton collisions at $\sqrt{s}$=13 TeV with the ATLAS detector
- Results compatible with SM predictions
- Moving from inclusive cross-section measurements to differential measurements
- Results with full LHC Run2 dataset are coming soon → Stay tuned !

# Additional material

# $t\bar{t}\gamma$ selection and pre-fit yields

- Single lepton and dilepton selections

| $e$+jets | $\mu$+jets | $ee$ | $\mu\mu$ | $e\mu$ |
|---|---|---|---|---|
| Primary vertex | | | | |
| 1 $e$ | 1 $\mu$ | 2 $e$, OS | 2 $\mu$, OS | 1 $e$ + 1 $\mu$, OS |
| Trigger match | | | | |
| $\geq$ 4 jets | | $\geq$ 2 jets | | |
| $\geq$ 1 $b$-jet | | | | |
| 1 $\gamma$ | | | | |
| $\lvert m(e,\gamma) - m(Z)\rvert > 5$ GeV | - | | | |
| - | | $m(\ell,\ell) \notin [85,95]$ GeV | | - |
| - | | $m(\ell,\ell,\gamma) \notin [85,95]$ GeV | | - |
| - | | $E_{\mathrm{T}}^{\mathrm{miss}} > 30$ GeV | | - |
| - | | $m(\ell,\ell) > 15$ GeV | | |
| $\Delta R(\gamma,\ell) > 1.0$ | | | | |

| Channel | Single lepton | Dilepton |
|---|---|---|
| $t\bar{t}\gamma$ | $6\,490 \pm 420$ | $720 \pm 34$ |
| Hadronic-fake | $1\,440 \pm 290$ | $49 \pm 27$ |
| Electron-fake | $1\,650 \pm 170$ | $2 \pm 1$ |
| Fake lepton | $360 \pm 200$ | – |
| $W\gamma$ | $1\,130$ | |
| $Z\gamma$ | | $75 \pm 52$ |
| Other prompt | $690 \pm 260$ | $18 \pm 7$ |
| Total | $11\,750 \pm 710$ | $863 \pm 78$ |
| Data | $11\,662$ | $902$ |

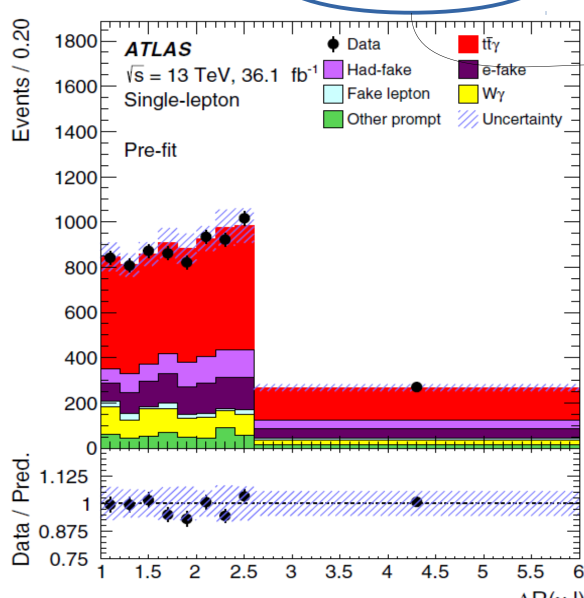


Reduce events where photon radiated by top decay products.

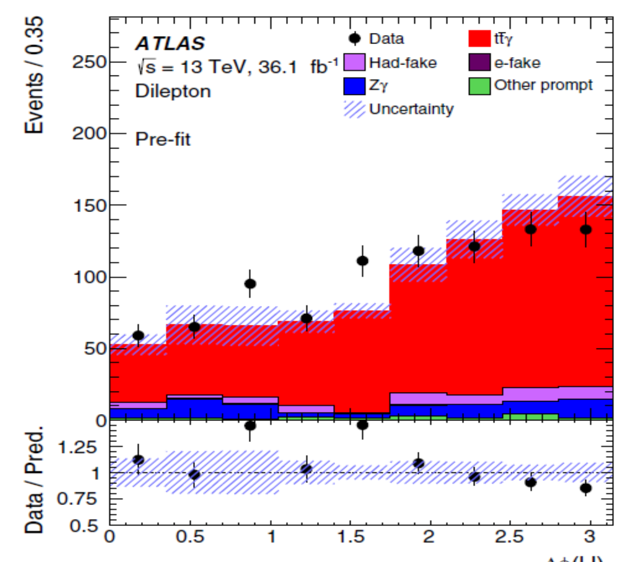


(e)

# Ttγ : event-level discriminator

- Prompt-photon tagger trained with shower shape variables: $R_\eta$, $R_\phi$, $w_{\eta 2}$, $w_{s3}$, $R_{had}$ and $F_{side}$

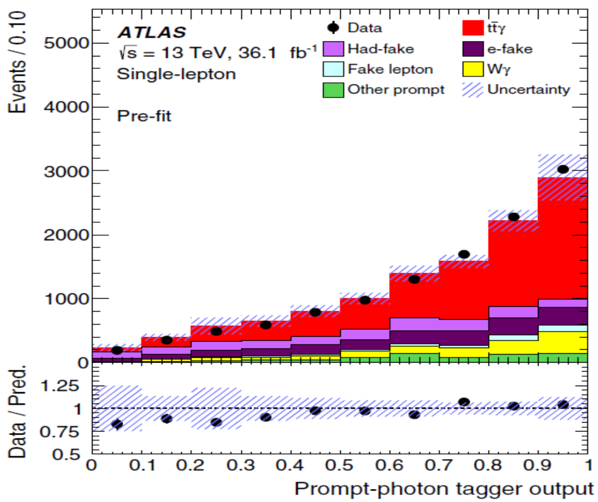


| Category | Description | Name |
|---|---|---|
| Acceptance | $\lvert\eta\rvert < 2.37$, with $1.37 < \lvert\eta\rvert < 1.52$ excluded | – |
| Hadronic leakage | Ratio of $E_T$ in the first sampling layer of the hadronic calorimeter to $E_T$ of the EM cluster (used over the range $\lvert\eta\rvert < 0.8$ or $\lvert\eta\rvert > 1.37$) | $R_{had_1}$ |
| | Ratio of $E_T$ in the hadronic calorimeter to $E_T$ of the EM cluster (used over the range $0.8 < \lvert\eta\rvert < 1.37$) | $R_{had}$ |
| EM Middle layer | Ratio of $3 \times 7$ $\eta \times \phi$ to $7 \times 7$ cell energies | $R_\eta$ |
| | Lateral width of the shower | $w_{\eta 2}$ |
| | Ratio of 3×3 $\eta \times \phi$ to 3×7 cell energies | $R_\phi$ |
| EM Strip layer | Shower width calculated from three strips around the strip with maximum energy deposit | $w_{s\,3}$ |
| | Total lateral shower width | $w_{s\,\mathrm{tot}}$ |
| | Energy outside the core of the three central strips but within seven strips divided by energy within the three central strips | $F_{\mathrm{side}}$ |

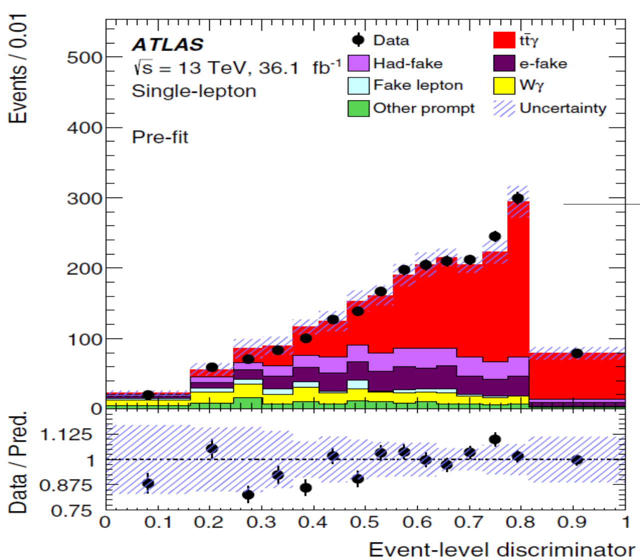


**Table 3** Input variables for the event-level discriminator for the single-lepton and dilepton channels. For events without the 5th jet, the $p_T(j_5)$ is set to zero

| Variable | Description | Single lepton | Dilepton |
|---|---|---|---|
| PPT | Prompt-photon tagger output | ✓ | |
| $H_T$ | Scalar sum of the $p_T$ of the leptons and jets | ✓ | |
| $m(\gamma, \ell)$ | Invariant mass of the system of the photon and the lepton | ✓ | |
| $E_T^{miss}$ | Missing transverse energy | ✓ | ✓ |
| $m_W^T$ | Reconstructed transverse mass of the leptonically decaying $W$-boson $= \sqrt{2 \times p_T(\ell) \times E_T^{miss} \times (1 - \cos(\Delta\phi(\ell, E_T^{miss})))}$ | ✓ | |
| $N_{jets}$ | Jet multiplicity | ✓ | |
| $p_T(j_1)$ | $p_T$ of the leading jet (ordered in $p_T$) | ✓ | ✓ |
| $p_T(j_2)$ | $p_T$ of the sub-leading jet | ✓ | ✓ |
| $p_T(j_3)$ | $p_T$ of the third jet | ✓ | |
| $p_T(j_4)$ | $p_T$ of the fourth jet | ✓ | |
| $p_T(j_5)$ | $p_T$ of the fifth jet | ✓ | |
| $N_{b\text{-jets}}$ | $b$-jet multiplicity | ✓ | ✓ |
| $b_1(j)$ | highest $b$-tagging score of all jets | ✓ | ✓ |
| $b_2(j)$ | second highest $b$-tagging score of all jets | ✓ | ✓ |
| $b_3(j)$ | third highest $b$-tagging score of all jets | ✓ | |
| $m(\ell, \ell)$ | Invariant mass of the system of the two leptons | | ✓ |

# ttγ differential measurements (single-lepton)

- Dominated in general by the modelling of the ttbar sample I most of the unfolded bins

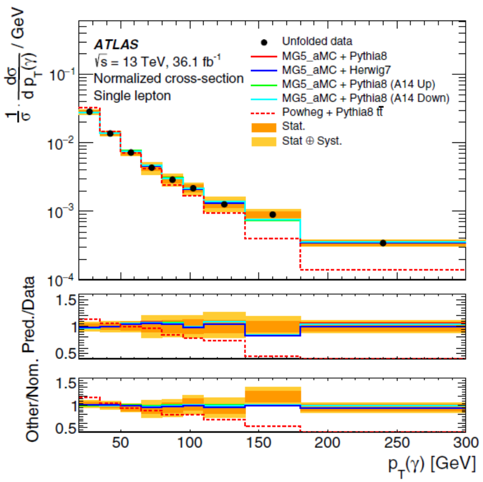

(a)

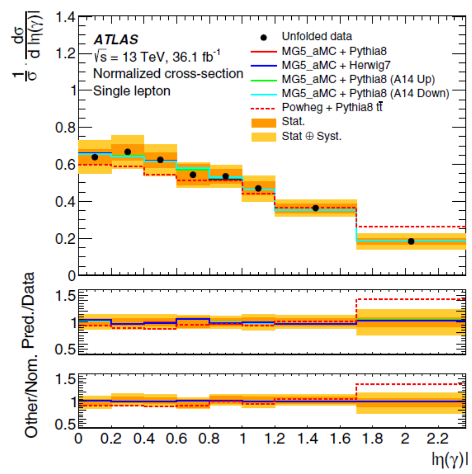

(b)

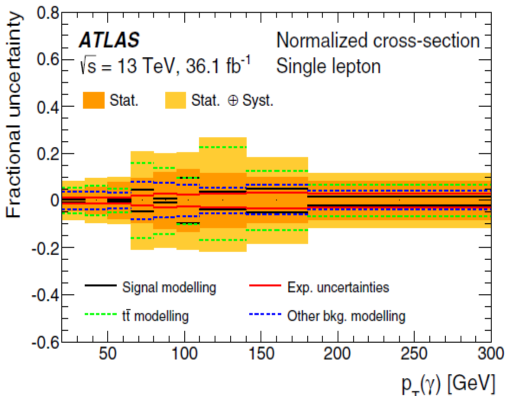

(a)

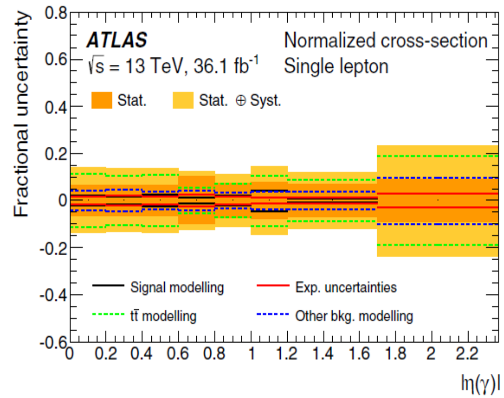

(b)

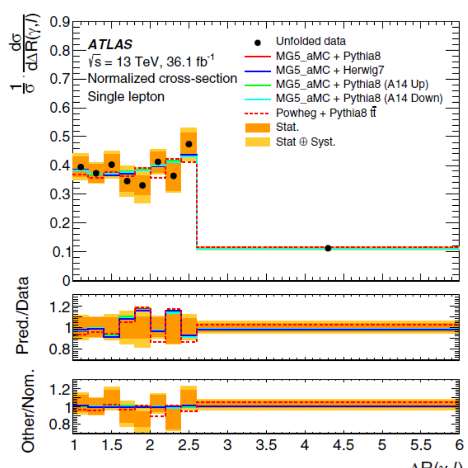

(c)

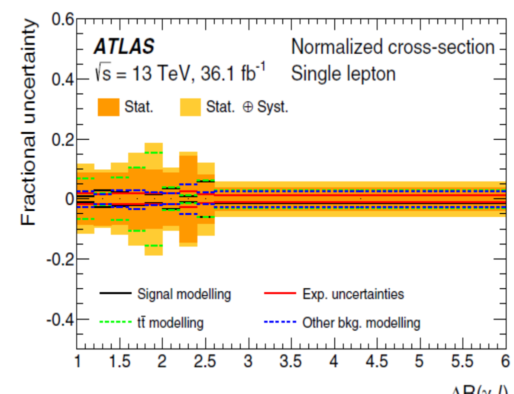

(c)

# $t\bar{t}W/t\bar{t}Z$ signal regions

## $t\bar{t}W$ signal regions

### 2L

| Requirement | $2\ell$-SS(p,m)-1$b$ | $2e$-SS(p,m)-2$b$ | $e\mu$-SS(p,m)-2$b$ | $2\mu$-SS(p,m)-2$b$ |
|---|---|---|---|---|
| $n_{b\text{-tags}}$ | =1 | ≥2 | ≥2 | ≥2 |
| $E_T^{miss}$ | >40 GeV | >40 GeV | >40 GeV | >20 GeV |
| $H_T$ | >240 GeV | | | |
| $p_T$ (leading lepton) | >27 GeV | | | |
| $p_T$ (subleading lepton) | >27 GeV | | | |
| $n_{jets}$ | ≥4 | ≥4 | ≥4 | ≥2 |
| $Z$ veto | $\|m_{\ell\ell} - m_Z\| > 10$ GeV in the $2e$ and $2\mu$ regions | | | |

### 3L

TABLE V. Summary of event selection requirements in the trilepton signal regions targeting the $t\bar{t}W$ process.

| Variable | $3\ell$p-noZ-2b2j | $3\ell$m-noZ-2b2j | $3\ell$p-noZ-1b2j | $3\ell$m-noZ-1b2j |
|---|---|---|---|---|
| All leptons | $p_T > 27$ GeV | | | |
| $Z$ veto (OSSF pair) | $\|m_{\ell\ell} - m_Z\| > 10$ GeV | | | |
| $n_{jets}$ | 2 or 3 | | | |
| $H_T$ | ... | | >240 GeV | |
| Sum of lepton charges | +1 | −1 | +1 | −1 |
| $n_{b\text{-tags}}$ | ≥2 | ≥2 | 1 | 1 |

## $t\bar{t}Z$ signal regions

### 2L

| Variable | $2\ell$-Z-6j1b | $2\ell$-Z-5j2b | $2\ell$-Z-6j2b |
|---|---|---|---|
| Leptons | =2, same flavor and opposite sign | | |
| $m_{\ell\ell}$ | $\|m_{\ell\ell} - m_Z\| < 10$ GeV | | |
| $p_T$ (leading lepton) | >30 GeV | | |
| $p_T$ (subleading lepton) | >15 GeV | | |
| $n_{b\text{-tags}}$ | 1 | ≥2 | ≥2 |
| $n_{jets}$ | ≥6 | 5 | ≥6 |

### 4L

| Region | $Z_2$ leptons | $p_{T4}$ | $p_{T34}$ | $\|m_{Z_2} - m_Z\|$ | $E_T^{miss}$ | $n_{b\text{-tags}}$ |
|---|---|---|---|---|---|---|
| $4\ell$-DF-1b | $e^\pm\mu^\mp$ | ... | >35 GeV | ... | ... | 1 |
| $4\ell$-DF-2b | $e^\pm\mu^\mp$ | >10 GeV | ... | ... | ... | ≥2 |
| $4\ell$-SF-1b | $e^\pm e^\mp, \mu^\pm\mu^\mp$ | ... | >25 GeV | >10 GeV | >40 GeV | 1 |
| | | | | <10 GeV | >80 GeV | |
| $4\ell$-SF-2b | $e^\pm e^\mp, \mu^\pm\mu^\mp$ | >10 GeV | ... | >10 GeV | ... | ≥2 |
| | | | | <10 GeV | >40 GeV | |

### 3L

| Variable | $3\ell$-Z-1b4j | $3\ell$-Z-2b3j | $3\ell$-Z-2b4j | $3\ell$-noZ-2b4j |
|---|---|---|---|---|
| Leading lepton | $p_T > 27$ GeV | | | |
| Other leptons | $p_T > 20$ GeV | | | |
| Sum of lepton charges | ±1 | | | |
| $Z$ requirement (OSSF pair) | $\|m_{\ell\ell} - m_Z\| < 10$ GeV | | | $\|m_{\ell\ell} - m_Z\| > 10$ GeV |
| $n_{jets}$ | ≥4 | 3 | ≥4 | ≥4 |
| $n_{b\text{-tags}}$ | 1 | ≥2 | ≥2 | ≥2 |

# ttγ differential measurement (dilepton)

- Dominanted by statistical uncertainties except for bins at high values, where the main background modelling dominates